

## Exploring three-dimensional implicit wavefield extrapolation with the helix transform

Sergey Fomel and Jon F. Claerbout<sup>1</sup>

### ABSTRACT

Implicit extrapolation is an efficient and unconditionally stable method of wavefield continuation. Unfortunately, implicit wave extrapolation in three dimensions requires an expensive solution of a large system of linear equations. However, by mapping the computational domain into one dimension via the helix transform, we show that the matrix inversion problem can be recast in terms of an efficient recursive filtering. Apart from the boundary conditions, the solution is exact in the case of constant coefficients (that is, a laterally homogeneous velocity.) We illustrate this fact with an example of three-dimensional velocity continuation and discuss possible ways of attacking the problem of lateral variations.

### INTRODUCTION

Implicit finite-difference wavefield extrapolation played an exceptionally important role in the early development of seismic migration methods. Using limited-degree approximations to the one-way wave equation, implicit schemes have provided efficient and unconditionally stable numerical wave extrapolation operators (Godfrey et al., 1979; Claerbout, 1985). Unfortunately, the advantages of *implicit* methods were lost with the development of three-dimensional seismic exploration. While the cost of 2-D implicit extrapolation is linearly proportional to the mesh size, the same approach, applied in the 3-D case, leads to a nonlinear computational complexity. Primarily for this reason, implicit extrapolators were replaced in practice by *explicit* ones, capable of maintaining linear complexity in all dimensions. A number of computational tricks (Hale, 1991b) allow the commonly used explicit schemes to behave stably in practical cases. However, their stability is not unconditional and may break in unusual situations (Etgen, 1994).

In this paper, we present an approach to three-dimensional extrapolation, based on the helix transform of multidimensional filters to one dimension (Claerbout, 1997b). The traditional approach involves an inversion of a banded matrix (tridiagonal in the 2-D case and blocked-tridiagonal in the 3-D case). With the help of the helix transform, we can recast this problem in terms of inverse recursive filtering. The coefficients of two-dimensional filters on a helix are obtained by one-dimensional spectral factorization methods. As a result, the complexity of

---

<sup>1</sup>email: sergey@sep.stanford.edu, jon@sep.stanford.edu

three-dimensional implicit extrapolation is reduced to a linear function of the computational mesh size. This approach doesn't provide an exact solution in the presence of lateral velocity variations. Nevertheless, it can be used for preconditioning iterative methods, such as those described by Nichols (1991). In this paper, we demonstrate the feasibility of 3-D implicit extrapolation on the example of laterally invariant velocity continuation and, in the final part, discuss possible strategies for solving the problem of lateral variations.

The main application of finite-difference wave extrapolation is *post-stack* depth migration. An application of similar methods for *prestack* common-shot migration is constrained by the limited aperture of commonly used seismic acquisition patterns. Recently developed acquisition methods, such as the vertical cable technique (Krail, 1993), open up new possibilities for 3-D wave extrapolation applications. An alternative approach is common-azimuth migration (Biondi and Palacharla, 1994; Biondi, 1996). Other interesting applications include finite-difference data extrapolation in offset (Fomel, 1995), migration velocity (Fomel, 1996a), and anisotropy (Alkhalifah and Fomel, 1997).

### IMPLICIT VERSUS EXPLICIT EXTRAPOLATION

The difference between implicit and explicit extrapolation is best understood through an example. Following Claerbout (1985), let us consider, for instance, the diffusion (heat conduction) equation of the form

$$\frac{\partial T}{\partial t} = a(x) \frac{\partial^2 T}{\partial x^2} . \quad (1)$$

Here  $t$  denotes time,  $x$  is the space coordinate,  $T(x, t)$  is the temperature, and  $a$  is the heat conductivity coefficient. Equation (1) forms a well-posed boundary-value problem if supplied with the initial condition

$$T|_{t=0} = T_0(x) \quad (2)$$

and the appropriate boundary conditions. Our task is to build a digital filter, which transforms a gridded temperature  $T$  from one time level to another.

It helps to note that when the conductivity coefficient  $a$  is constant and the space domain of the problem is infinite (or periodic) in  $x$ , the problem can be solved in the wavenumber domain. Indeed, after the Fourier transform over the variable  $x$ , equation (1) transforms to the ordinary differential equation

$$\frac{d\hat{T}}{dt} = -ak^2 \hat{T} , \quad (3)$$

which has the explicit analytical solution

$$\hat{T}(k, t) = \hat{T}_0(k) e^{-ak^2 t} , \quad (4)$$

where  $\hat{T}$  denotes the Fourier transform of  $T$ , and  $k$  stands for the wavenumber. Therefore, the desired filter in the wavenumber domain has the form

$$H(k) = e^{-ak^2}, \tag{5}$$

where for simplicity the coefficient  $a$  is normalized for the time step  $\Delta t$  equal to 1.

Returning now to the time-and-space domain, we can approach the filter construction problem by approximating the space-domain response of filter (5) in terms of the differential operators  $\frac{\partial^2}{\partial x^2} = -k^2$ , which can be approximated by finite differences. An *explicit* approach would amount to constructing a series expansion of the form

$$H_{\text{ex}}(k) \approx a_0 + a_1k^2 + a_2k^4 + \dots, \tag{6}$$

and selecting the coefficients  $a_j$  to approximate equation (5). For example, the three-term Taylor series expansion around the zero wavenumber yields

$$H_{\text{ex}}(k) = 1 - ak^2 + \frac{a^2k^4}{2}. \tag{7}$$

The error of approximation (7) as a function of  $k$  for two different values of  $a$  is shown in the left plot of Figure 1.

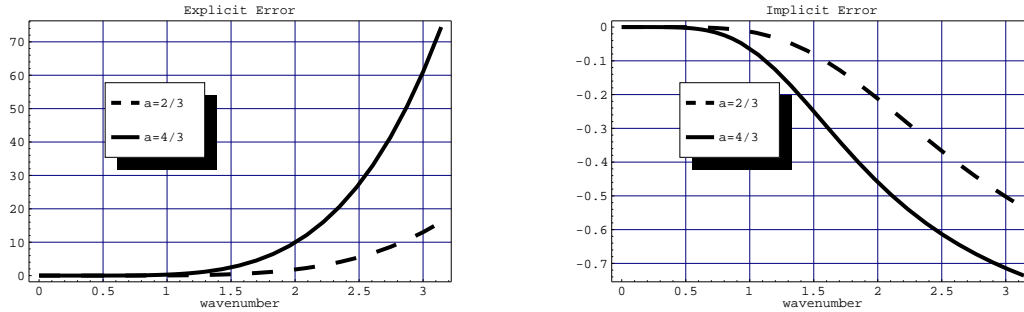


Figure 1: Errors of second-order explicit and implicit approximations for the heat extrapolation. `findif-error` [CR]

An *implicit* approach also approximates the ideal filter (5), but with a rational approximation of the form

$$H_{\text{im}}(k) \approx \frac{b_0 + b_1k^2 + b_2k^4 + \dots}{1 + c_1k^2 + c_2k^4 + \dots}. \tag{8}$$

One way of selecting the coefficients  $b_i$  and  $c_i$  is to apply an appropriate Padé approximation (Baker and Graves-Morris, 1981)<sup>2</sup>. For example the [2/2] Padé approximation is

$$H_{\text{im}}(k) = \frac{1 - \frac{a}{2}k^2}{1 + \frac{a}{2}k^2}. \tag{9}$$

<sup>2</sup>If the denominator and the numerator have the same order, Padé approximants are equivalent to the corresponding continuous fraction expansions.

This approximation corresponds to the famous Crank-Nicolson implicit method (Crank and Nicolson, 1947). The error of approximation (9) as a function of  $k$  for different values of  $a$  is shown in the right plot of Figure 1. Not only is it significantly smaller than the error of the same-order explicit approximation, but it also has a negative sign. It means that the high-frequency numerical noise gets suppressed rather than amplified. In practice, this property translates into a stable numerical extrapolation.

The second derivative operator  $-k^2$  can be approximated in practice by a digital filter. The most commonly used filter has the  $Z$ -transform  $D_2(Z) = -Z^{-1} + 2 - Z$ , and the Fourier transform

$$D_2(k) = e^{-ik} - 2 + e^{ik} = 2(\cos k - 1) = -4 \sin^2 \frac{k}{2}. \quad (10)$$

Formula (10) approximates  $-k^2$  well only for small wavenumbers  $k$ . As shown in Appendix A, the implicit scheme allows the accuracy of the second-derivative filter to be significantly improved by a variation of the “1/6-th trick” (Claerbout, 1985). The final form of the implicit extrapolation filter is

$$H_{\text{im}}(k) = \frac{1 + \frac{a+\beta}{2} D_2(k)}{1 - \frac{a-\beta}{2} D_2(k)}, \quad (11)$$

where  $\beta$  is a numerical constant, found in Appendix A.

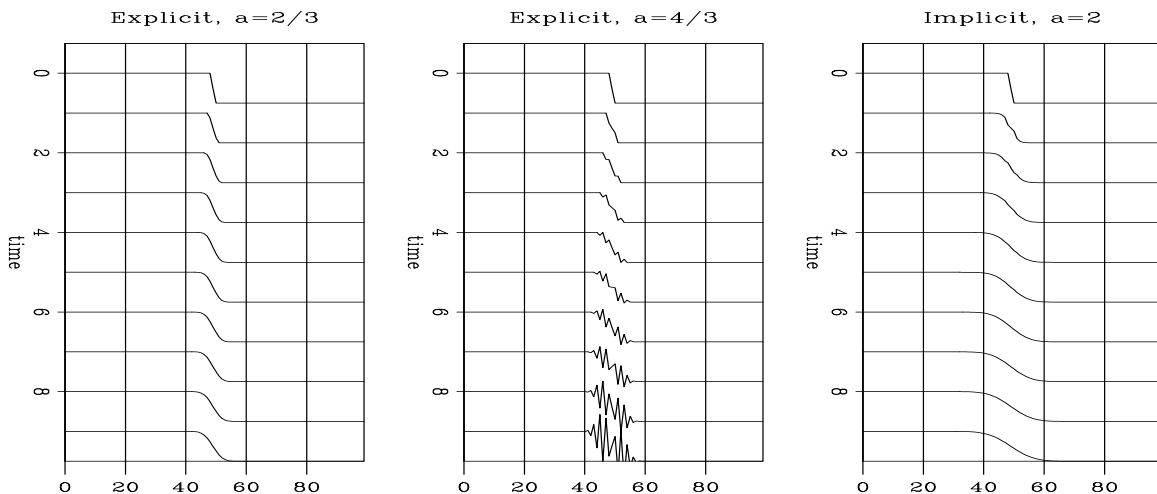


Figure 2: Heat extrapolation with explicit and implicit finite-difference schemes. Explicit extrapolation appears stable for  $a = 2/3$  (left plot) and unstable for  $a = 4/3$  (middle plot). Implicit interpolation is stable even for larger values of  $a$  (right plot). `findif-heat` [ER]

A numerical 1-D example is shown in Figure 2. The initial temperature distribution is given by a step function. The discontinuity at the step gets smoothed with time by the heat diffusion. The left plot shows the result of an explicit extrapolation with  $a = 2/3$ , which appears stable. The middle plot is an explicit extrapolation with  $a = 4/3$ , which shows a terribly unstable behavior: the high-frequency numerical noise is amplified and dominates the

solution. The right plot shows a stable (though not perfectly accurate) extrapolation with the implicit scheme for the larger value of  $a = 2$ .

The difference in stability between explicit and implicit schemes is even more pronounced in the case of *wave extrapolation*. For example, let us consider the ideal depth extrapolation filter in the form of the phase-shift operator (Gazdag, 1978; Claerbout, 1985)

$$W(k) = e^{i\sqrt{a^2-k^2}}, \tag{12}$$

where  $a = \omega/v$ ,  $\omega$  is the time frequency, and  $v$  is the seismic velocity (which may vary spatially); we assume for simplicity that both the depth step  $\Delta z$  and the space sampling  $\Delta x$  are normalized to 1. A simple implicit approximation to filter (12) is

$$W_{\text{im}}(k) = e^{ia} \frac{1 - 4a^2 + ia k^2}{1 - 4a^2 - ia k^2} = e^{i\phi}, \tag{13}$$

where  $\phi = a - 2 \arctan \frac{ak^2}{4a^2-1}$ . We can see that approximation (13) is again a pure phase shift operator, only with a slightly different phase. For that reason, the operator is unconditionally stable for all values of  $a$ : the total wave energy from one depth level to another is preserved. Operator (12) corresponds to the Crank-Nicolson scheme for the 45-degree one-way wave equation (Claerbout, 1985). Its phase error as a function of the dip angle  $\theta = \arcsin \frac{k}{a}$  for different values of  $a$  is shown in Figure 3.

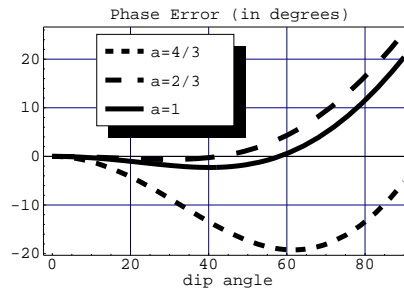


Figure 3: The phase error of the implicit depth extrapolation with the Crank-Nicolson method.

`findif-phase` [CR]

The unconditional stability property is not achievable with the explicit approach, though it is possible to increase the stability of explicit operators by using relatively long filters (Holberg, 1988; Hale, 1991b).

### SPECTRAL FACTORIZATION AND THREE-DIMENSIONAL EXTRAPOLATION

In this section, we continue our review of extrapolation methods to reveal the principal difficulties of three-dimensional extrapolation. We then describe a new, helix-transform approach to this old and fascinating problem.

#### Inverse filter factorization

The conventional way of applying implicit finite-difference schemes reduces to solving a system of linear equations with a sparse matrix. For example, to apply the scheme of equation

(11), we can put the filter denominator on the other side of the extrapolation equation, writing it as

$$\left(\mathbf{I} - \frac{a - \beta}{2} \mathbf{D}_2\right) \mathbf{T}_{t+1} = \left(\mathbf{I} + \frac{a + \beta}{2} \mathbf{D}_2\right) \mathbf{T}_t, \quad (14)$$

where  $\mathbf{I}$  is the identity matrix,  $\mathbf{D}$  is the convolution matrix for filter (10), and  $\mathbf{T}_t$  is the vector of temperature distribution at time level  $t$ . In the case of two-dimensional extrapolation, the matrix on the left side of equation (14) takes the tridiagonal form

$$\mathbf{A} = (\mathbf{I} - c \mathbf{D}_2) = \begin{bmatrix} 1 + 2c_1 & -c_1 & 0 & \cdots & & 0 \\ -c_2 & 1 + 2c_2 & -c_2 & 0 & \cdots & \\ 0 & -c_3 & \cdots & \cdots & & \cdots \\ \cdots & 0 & \cdots & & & \\ & \cdots & & & \cdots & -c_{n-1} \\ 0 & & & & -c_n & 1 + 2c_n \end{bmatrix}, \quad (15)$$

where  $c = \frac{a - \beta}{2}$ , and where, for simplicity, we assume zero-slope boundary conditions. Like any positive-definite tridiagonal matrix, matrix  $\mathbf{A}$  can be inverted recursively by an  $LU$  decomposition into two bidiagonal matrices. The cost of inversion is directly proportional to the number of vector components. The same conclusion holds for the case of depth extrapolation [equation (13)] with the substitution  $c = \frac{\beta + ia}{1 - 4a^2}$ .

In the case of a laterally constant coefficient  $a$ , we can take a different point of view on the tridiagonal matrix inversion. In this case, the matrix  $\mathbf{A}_2$  represents a convolution with a symmetric three-point filter  $1 - c D_2(k)$ . The  $LU$  decomposition of such a matrix is precisely equivalent to filter *factorization* into the product of a causal minimum-phase filter with its adjoint. This conclusion can be confirmed by the easily verified equality

$$1 + c(Z^{-1} - 2 + Z) = \frac{(1 + b)^2}{4} \left(1 + \frac{1 - b}{1 + b} Z\right) \left(1 + \frac{1 - b}{1 + b} Z^{-1}\right), \quad (16)$$

where  $b = \sqrt{1 + 4c}$ . The inverse of the causal minimum-phase filter  $1 + \frac{1 - b}{1 + b} Z$  is a recursive inverse filter. Correspondingly, the inverse of its adjoint pair,  $1 + \frac{1 - b}{1 + b} Z^{-1}$ , is the same inverse filtering, performed in the adjoint mode (backwards in space). In the next subsection, we show how this approach can be carried into three dimensions by applying the helix transform.

### Helix and multidimensional deconvolution

The major obstacle of applying an implicit extrapolation in three dimensions is that the inverted matrix is no longer tridiagonal. If we approximate the second derivative (Laplacian) on the 2-D plane with the commonly used five-point filter  $Z_x^{-1} + Z_y^{-1} - 4 + Z_x + Z_y$ , then the matrix on the left side of equation (14), under the usual mapping of vectors from a two-dimensional mesh to one dimension, takes the infamous blocked-tridiagonal form (Birkhoff,

1971)

$$\tilde{\mathbf{A}} = (\mathbf{I} - c\mathbf{D}_2) = \begin{bmatrix} \mathbf{A}_1 & -c_1\mathbf{I} & 0 & \cdots & & 0 \\ -c_2\mathbf{I} & \mathbf{A}_2 & -c_2\mathbf{I} & 0 & \cdots & \\ 0 & -c_3\mathbf{I} & \cdots & \cdots & & \cdots \\ \cdots & 0 & \cdots & & & \\ & \cdots & & & \cdots & -c_{n-1}\mathbf{I} \\ 0 & & & & -c_n\mathbf{I} & \mathbf{A}_n \end{bmatrix}. \quad (17)$$

Inspecting this form more closely, we see that the main diagonal of  $\tilde{\mathbf{A}}$ , as well as the two offset diagonals formed by the scaled identity matrices, remains continuous, while the second top and bottom diagonals are broken. Therefore, even for constant  $c$ , the inverted matrix does not have a simple convolutional structure, and the cost of its inversion grows nonlinearly with the number of grid points.

A *helix transform*, recently proposed by one of the authors (Claerbout, 1997a), sheds new light on this old problem. Let us assume that the extrapolation filter is applied by sliding it along the  $x$  direction in the  $\{x, y\}$  plane. The diagonal discontinuities in matrix  $\tilde{\mathbf{A}}$  occur exactly in the places where the forward leg of the filter slides outside the computational domain. Let's imagine a situation, where the leg of the filter that went to the end of the  $x$  column, would immediately appear at the beginning of the next column. This situation defines a different mapping from two computational dimensions to the one dimension of linear algebra. The mapping can be understood as the helix transform, illustrated in Figure 4 and explained in detail by Claerbout (1997a). According to this transform, we replace the original two-dimensional filter with a long one-dimensional filter. The new filter is partially filled with zero values (corresponding to the back side of the helix), which can be safely ignored in the convolutional computation.

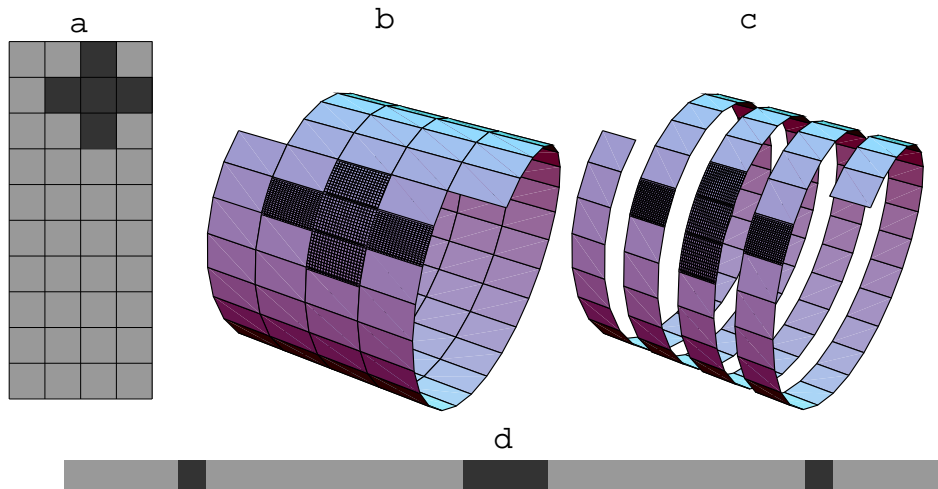


Figure 4: The helix transform of two-dimensional filters to one dimension. The two-dimensional filter in the left plot is equivalent to the one-dimensional filter in the right plot, assuming that a shifted periodic condition is imposed on one of the axes. [findif-helix1](#) [CR]

This is exactly the helix transform that is required to make all the diagonals of matrix  $\tilde{\mathbf{A}}$  continuous. In the case of laterally invariant coefficients, the matrix becomes strictly Toeplitz (having constant values along the diagonals) and represents a one-dimensional convolution on the helix surface. Moreover, this simplified matrix structure applies equally well to larger second-derivative filters (such as those described in Appendix B), with the obvious increase of the number of Toeplitz diagonals. Inverting matrix  $\tilde{\mathbf{A}}$  becomes once again a simple inverse filtering problem. To decompose the 2-D filter into a pair consisting of a causal minimum-phase filter and its adjoint, we can apply spectral factorization methods from the 1-D filtering theory (Claerbout, 1976, 1992), for example, Kolmogorov's highly efficient method (Kolmogorov, 1939). Thus, in the case of a laterally invariant implicit extrapolation, matrix inversion reduces to a simple and efficient recursive filtering, which we need to run twice: first in the forward mode, and second in the adjoint mode.

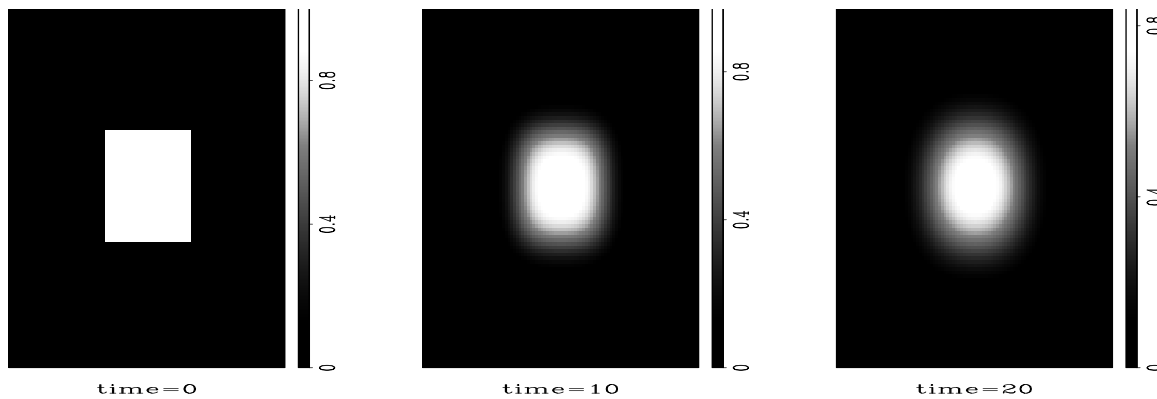
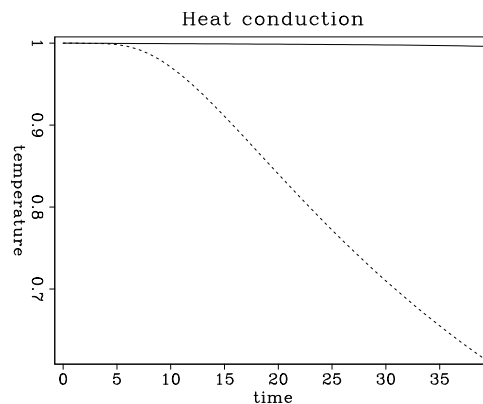


Figure 5: Heat extrapolation in two dimensions, computed by an implicit scheme with helix recursive filtering. The left plot shows the input temperature distributions; the two other plots, the extrapolation result at different time steps. The coefficient  $a$  is 2. `findif-heat3d` [ER]

Figure 5 shows the result of applying the helix transform to an implicit heat extrapolation of a two-dimensional temperature distribution. The unconditional stability properties are nicely preserved, which can be verified by examining the plot of changes in the average temperature (Figure 6).

Figure 6: Demonstration of the stability of implicit extrapolation. The solid curve shows the normalized mean temperature, which remains nearly constant throughout the extrapolation time. The dashed curve shows the normalized maximum value, which exhibits the expected Gaussian shape. `findif-heat-mean` [ER]



In principle, we could also treat the case of a laterally invariant coefficient with the help of



the Fourier transform. Under what circumstances does the helix approach have an advantage over Fourier methods? One possible situation corresponds to a very large input data size with a relatively small extrapolation filter. In this case, the  $O(N \log N)$  cost of the fast Fourier transform is comparable with the  $O(N_f N)$  cost of the space-domain deconvolution (where  $N$  corresponds to the data size, and  $N_f$  is the filter size). Another situation is when the boundary conditions of the problem have an essential lateral variation. The latter case may occur in applications of velocity continuation, which we discuss in the next section. Later in this paper, we return to the discussion of problems associated with lateral variations.

### THREE-DIMENSIONAL IMPLICIT VELOCITY CONTINUATION

Velocity continuation is a process of navigating in the migration velocity space, applicable for time migration, residual migration, and migration velocity analysis (Fomel, 1996a). In the zero-offset (post-stack) case, the velocity continuation process is described by the simple partial differential equation (Claerbout, 1986; Fomel, 1994)

$$\frac{\partial^2 P}{\partial v \partial t} + vt \left( \frac{\partial^2 P}{\partial x^2} + \frac{\partial^2 P}{\partial y^2} \right) = 0, \tag{18}$$

where  $t$  is the vertical time coordinate of the migrated image,  $x$  and  $y$  are spatial (midpoint) coordinates, and  $v$  is the migration velocity. Slightly different versions of two-dimensional implicit extrapolation with equation (18) have been described by Li (1986) and (Fomel, 1996a).

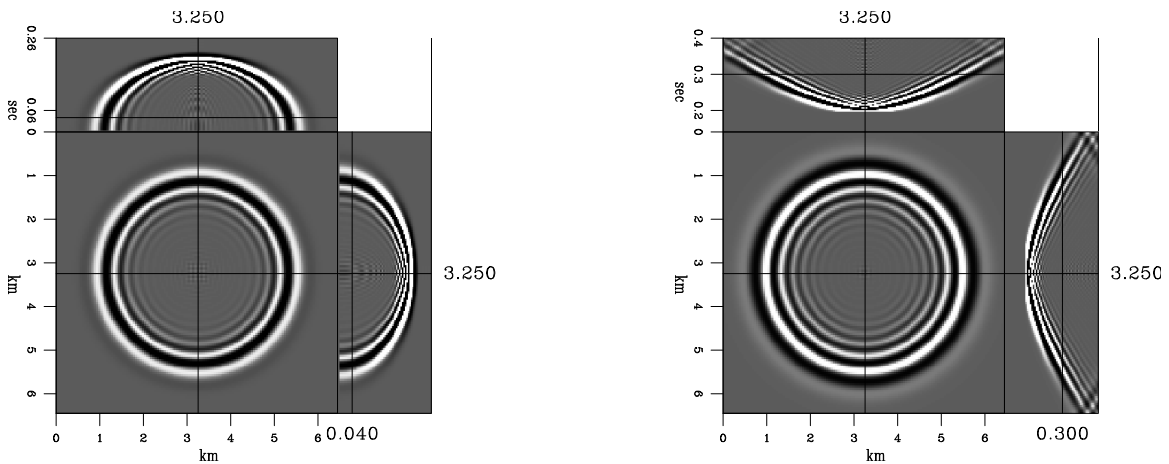


Figure 7: Impulse responses of the velocity continuation operator, computed by an implicit, unconditionally stable extrapolation via the helix transform. The left plot corresponds to continuation towards higher velocities (migration mode); the right plot, smaller velocities (modeling mode). `findif-velcon` [ER]

The helix approach has allowed us to modify the old code for three dimensions. Figure 7 shows impulse responses of an implicit helix-based three-dimensional velocity continuation.

Figure 8: Qdome synthetic model, used for testing the 3-D velocity continuation program. `findif-qdome` [ER]

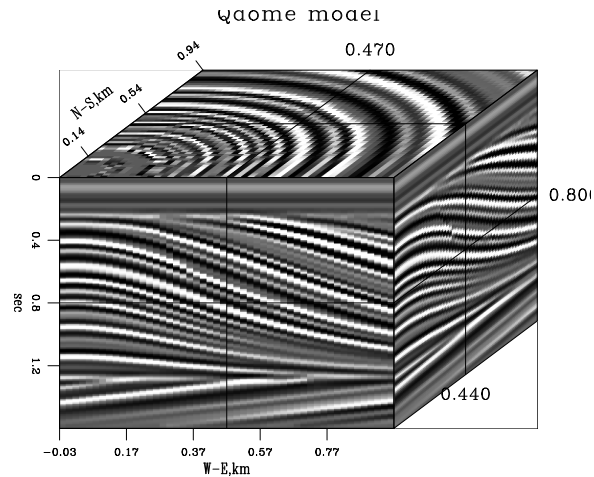


Figure 9 illustrates the velocity continuation process on the Qdome synthetic model (Claerbout, 1997b), shown in Figure 8. Continuation backward in velocity corresponds to the “modeling” mode, while forward continuation corresponds to the “migration” mode. It is possible to balance the amplitudes of the two processes so that the finite-difference velocity continuation behaves as a unitary operator (Fomel, 1996a,b).

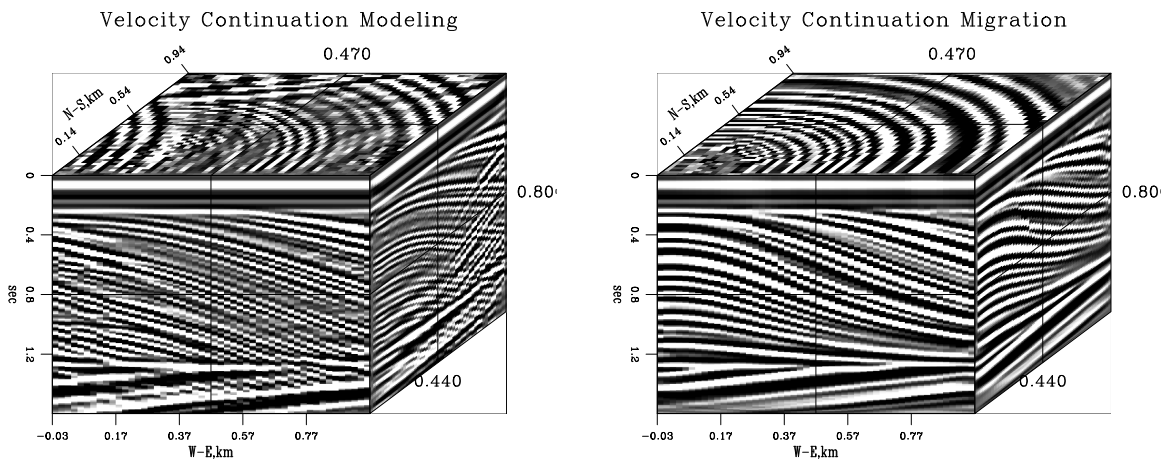


Figure 9: Modeling (left) and migration (right) with the Qdome synthetic model, obtained by running the 3-D velocity continuation backward and forward in velocity. `findif-modmig` [CR]

## DEPTH EXTRAPOLATION AND THE $V(X)$ CHALLENGE

Can the constant-velocity result help us achieve the challenging goal of a stable implicit depth extrapolation through media with lateral velocity variations?

The first idea that comes to mind is to replace the space-invariant helix filters with a pre-computed set of spatially varying filters, which reflect local changes in the velocity fields.

This approach would merely reproduce the conventional practice of explicit depth extrapolators, popularized by Holberg (1988) and Hale (1991b). However, it hides the danger of losing the property of unconditional stability, which is obviously the major asset of implicit extrapolators.

Another route, partially explored by Nichols (1991), is to implement the matrix inversion in the three-dimensional implicit scheme by an iterative method. In this case, the helix inversion may serve as a powerful preconditioner, providing an immediate answer in constant velocity layers and speeding up the convergence in the case of velocity variations. To see why this might be true, one can write the variable-coefficient matrix  $\tilde{\mathbf{A}}$  in the form

$$\tilde{\mathbf{A}} = \mathbf{B} + \mathbf{D}, \quad (19)$$

where matrix  $\mathbf{B}$  corresponds to some constant average velocity, and  $\mathbf{D}$  is the matrix of velocity perturbations. The system of linear equations that we need to solve is then

$$(\mathbf{B} + \mathbf{D})\mathbf{m} = \mathbf{d}, \quad (20)$$

where  $\mathbf{m}$  is the vector of extrapolated wavefield, and  $\mathbf{d}$  is an appropriate righthand side. The helix transform provides us with the operator  $\mathbf{B}^{-1}$ , which we can use to precondition system (20). Introducing the change of variables

$$\mathbf{m} = \mathbf{B}^{-1}\mathbf{x}, \quad (21)$$

we can transform the original system (20) to the form

$$\mathbf{d} = (\mathbf{B} + \mathbf{D})\mathbf{B}^{-1}\mathbf{x} = \mathbf{x} + \mathbf{D}\mathbf{B}^{-1}\mathbf{x}. \quad (22)$$

When the velocity perturbation is small<sup>3</sup>, even the simple iteration

$$\mathbf{x}_0 = \mathbf{d}; \quad (23)$$

$$\mathbf{x}_k = \mathbf{d} - \mathbf{D}\mathbf{B}^{-1}\mathbf{x}_{k+1} \quad (24)$$

will converge rapidly to the desired solution. This interesting possibility needs thorough testing.

The third untested possibility (Papanicolaou, personal communication) is to implement a clever patching in the velocity domain, applying a constant-velocity filter locally inside each patch. Recently developed fast wavelet transform techniques (Vetterli and Kovacevic, 1995), in particular the *local cosine transform*, provide a formal framework for that approach.

## CONCLUSIONS

The feasibility of multidimensional deconvolution, proven by the helix transform, allows us to revisit the problem of implicit wavefield extrapolation in three dimensions. The attraction

<sup>3</sup>In the linear-algebraic sense, this means that the spectral radius of operator  $\mathbf{D}\mathbf{B}^{-1}$  is strictly less than one.

of implicit finite-difference methods lies in their unconditional stability, a property invaluable for practical applications.

We have shown that at least in the constant coefficient case (that is, laterally invariant velocity), it is possible to implement an extremely efficient implicit extrapolation by a recursive inverse filtering in the helix-transformed computational model. Unfortunately, the case of lateral velocity variations still presents a difficult problem that may not have an exact solution. We are currently exploring different roads to that goal.

### ACKNOWLEDGMENTS

We thank Biondo Biondi for useful discussions and for sharing his three-dimensional expertise.

### REFERENCES

- Alkhalifah, T., and Fomel, S., 1997, Residual migration in VTI media using anisotropy continuation: *SEP-94*, 327–337.
- Baker, G. A., and Graves-Morris, P., 1981, *Padé approximants*: Addison-Wesley.
- Biondi, B., and Palacharla, G., 1993, 3-D wavefield depth extrapolation by rotated McClellan filters: *SEP-77*, 27–36.
- Biondi, B., and Palacharla, G., 1994, 3-D prestack migration of common-azimuth data: *SEP-80*, 109–124.
- Biondi, B., 1996, Common-azimuth prestack depth migration of a North Sea data set: *SEP-93*, 1–14.
- Birkhoff, G., 1971, *The numerical solution of elliptic equations*: SIAM, Philadelphia.
- Claerbout, J. F., 1976, *Fundamentals of geophysical data processing*: Blackwell.
- Claerbout, J. F., 1985, *Imaging the Earth's Interior*: Blackwell Scientific Publications.
- Claerbout, J. F., 1986, Velocity extrapolation by cascaded 15 degree migration: *SEP-48*, 79–84.
- Claerbout, J. F., 1992, *Earth Soundings Analysis: Processing Versus Inversion*: Blackwell Scientific Publications.
- Claerbout, J., 1997a, Multidimensional recursive filters via a helix: *SEP-95*, 1–13.
- Claerbout, J. F., 1997b, *Geophysical exploration mapping: Environmental soundings image enhancement*: Stanford Exploration Project.

- Cole, J. B., 1994, A nearly exact second-order finite-difference time-domain wave propagation algorithm on a coarse grid: *Computers in Physics*, **8**, no. 6.
- Crank, J., and Nicolson, P., 1947, A practical method for numerical evaluation of solutions of partial differential equations of the heat-conduction type: *Proceedings of the Cambridge Philosophical Society*, **43**, 50–67.
- Etgen, J. T., 1994, Stability of explicit depth extrapolation through laterally varying media: 64th Annual Internat. Mtg., Soc. Expl. Geophys., Expanded Abstracts, 1266–1269.
- Fomel, S. B., 1994, Method of velocity continuation in the problem of seismic time migration: *Russian Geology and Geophysics*, **35**, no. 5, 100–111.
- Fomel, S., 1995, Amplitude preserving offset continuation in theory Part 1: The offset continuation equation: *SEP*–**84**, 179–198.
- Fomel, S., 1996a, Migration and velocity analysis by velocity continuation: *SEP*–**92**, 159–188.
- Fomel, S., 1996b, Stacking operators: Adjoint versus asymptotic inverse: *SEP*–**92**, 267–292.
- Gazdag, J., 1978, Wave equation migration with the phase-shift method: *Geophysics*, **43**, no. 7, 1342–1351.
- Godfrey, R. J., Muir, F., and Claerbout, J. F., 1979, Stable extrapolation: *SEP*–**16**, 83–87.
- Hale, D., 1991a, 3-D Depth migration via McClellan transformations: *Geophysics*, **56**, no. 11, 1778–1785.
- Hale, D., 1991b, Stable explicit depth extrapolation of seismic wavefields: *Geophysics*, **56**, no. 11, 1770–1777.
- Holberg, O., 1988, Towards optimum one-way wave propagation: *Geophys. Prosp.*, **36**, no. 2, 99–114.
- Kolmogorov, A. N., 1939, Sur l'interpolation et l'extrapolation des suites stationnaires: *C.R. Acad.Sci.*, **208**, 2043–2045.
- Krail, P. M., 1993, Sub-salt acquisition with a vertical cable: 63rd Annual Internat. Mtg., Soc. Expl. Geophys., Expanded Abstracts, 1376.
- Li, Z., 1986, Cascaded one step fifteen degree migration versus Stolt migration: *SEP*–**48**, 85–100.
- McClellan, J. H., 1973, The design of two-dimensional digital filters by transformations: 7th Annual Princeton Conf. on Inform. Sci. and Syst., Proceedings, 247–251.
- Nichols, D., 1991, Three-dimensional depth migration by a predictor corrector method: *SEP*–**70**, 31–38.
- Vetterli, M., and Kovacevic, J., 1995, *Wavelets and subband coding*: Prentice Hall.

APPENDIX A

THE 1/6-TH TRICK

Given the filter  $D_2(k)$ , defined in formula (10), we can construct an accurate approximation to the second derivative operator  $-k^2$  by considering a filter ratio (another Padé-type approximation) of the form

$$-k^2 \approx \frac{D_2(k)}{1 + \beta D_2(k)}, \tag{A-1}$$

where  $\beta$  is an adjustable constant (Claerbout, 1985). The actual Padé coefficient is  $\beta = 1/12$ . As pointed out by Francis Muir, the value of  $\beta = 1/4 - 1/\pi^2 \approx 1/6.726$  gives an exact fit at the Nyquist frequency  $k = \pi$ . Fitting the derivative operator in the  $L_1$  norm yields the value of  $\beta \approx 1/8.13$ . All these approximations are shown in Figure A-1.

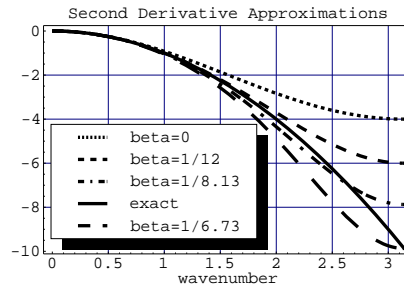


Figure A-1: The second-derivative operator in the wavenumber domain and its approximations. findif-sixth [CR]

APPENDIX B

CONSTRUCTING AN “ISOTROPIC” LAPLACIAN OPERATOR

The problem of approximating the Laplacian operator in two dimensions not only inherits the inaccuracies of the one-dimensional finite-difference approximations, but also raises the issue of azimuthal asymmetry. For example, the usual five-point filter

$$F_5 = \begin{bmatrix} 0 & 1 & 0 \\ 1 & -4 & 1 \\ 0 & 1 & 0 \end{bmatrix} \tag{B-1}$$

exhibits a clear difference between the grid directions and the directions at a 45-degree angle to the grid. To overcome this unpleasant anisotropy, we can consider a slightly larger filter of the form

$$F_9 = \begin{bmatrix} \alpha & & \gamma & \alpha \\ \gamma & -4(\alpha + \gamma) & & \gamma \\ \alpha & & \gamma & \alpha \end{bmatrix} \tag{B-2}$$

where the constants  $\alpha$  and  $\gamma$  are to be defined. The Fourier-domain representation of filter (B-2) is

$$F_9(k_x, k_y) = 4\alpha [\cos k_x \cos k_y - 1] + 2\gamma [\cos k_x + \cos k_y - 2], \quad (\text{B-3})$$

and the isotropic filter that we can try to approximate is defined analogously to its one-dimensional equivalent, as follows:

$$F(k_x, k_y) = 2(\cos k - 1) = 2(\cos \sqrt{k_x^2 + k_y^2} - 1). \quad (\text{B-4})$$

Comparing equations (B-3) and (B-4), we notice that they match exactly, when either of the wavenumbers  $k_x$  or  $k_y$  is equal to zero, provided that

$$\alpha = \frac{1 - \gamma}{2}. \quad (\text{B-5})$$

Therefore, we can reduce the problem to estimating a single coefficient  $\gamma$ . Another way of expressing this conclusion is to represent filter  $F_9$  in equation (B-3) as a linear combination of filter  $F_5$  from equation (B-3) and its rotated version (Cole, 1994), as follows:

$$F_9 = \gamma \begin{bmatrix} 0 & 1 & 0 \\ 1 & -4 & 1 \\ 0 & 1 & 0 \end{bmatrix} + (1 - \gamma) \begin{bmatrix} 1/2 & 0 & 1/2 \\ 0 & -2 & 0 \\ 1/2 & 0 & 1/2 \end{bmatrix} \quad (\text{B-6})$$

With the value of  $\gamma = 0.5$ , filter  $F_9$  takes the value

$$F_9 = \begin{bmatrix} 1/4 & 1/2 & 1/4 \\ 1/2 & -3 & 1/2 \\ 1/4 & 1/2 & 1/4 \end{bmatrix} \quad (\text{B-7})$$

and corresponds precisely to the nine-point McClellan filter (McClellan, 1973; Hale, 1991a). On the other hand, the value of  $\gamma = 2/3$  gives the least error in the vicinity of the zero wavenumber  $k$ . In this case, the filter is

$$F_9 = \begin{bmatrix} 1/6 & 2/3 & 1/6 \\ 2/3 & -10/3 & 2/3 \\ 1/6 & 2/3 & 1/6 \end{bmatrix} \quad (\text{B-8})$$

Errors of different approximations are plotted in Figure B-1<sup>4</sup>

Under the helix transform, a filter of the general form (B-2) becomes equivalent to a one-dimensional filter with the  $Z$  transform

$$F_9(Z) = \alpha Z^{-N_x-1} + \gamma Z^{-N_x} + \alpha Z^{-N_x+1} + \gamma Z^{-1} - 4(\alpha + \gamma) + \gamma Z + \alpha Z^{N_x-1} + \gamma Z^{N_x} + \alpha Z^{N_x+1}, \quad (\text{B-9})$$

<sup>4</sup>Another way of constructing circular-symmetric filters is suggested by the rotated McClellan transform (Biondi and Palacharla, 1993).

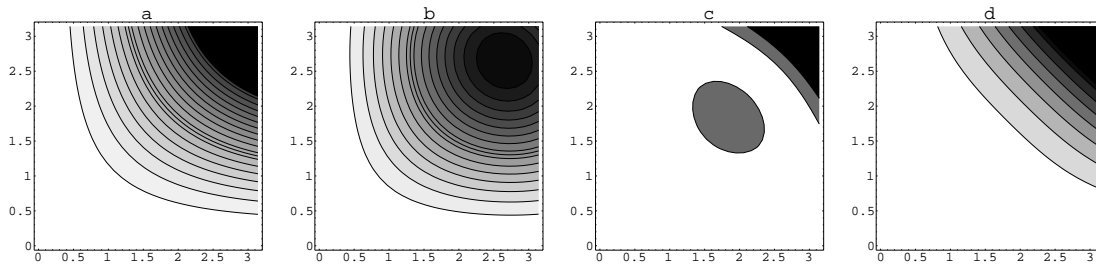


Figure B-1: The numerical anisotropy error of different Laplacian approximations. Both the five-point Laplacian (plot a) and its rotated version (plot b) are accurate along the axes, but exhibit significant anisotropy in between at large wavenumbers. The nine-point McClellan filter (plot c) has a reduced error, while the filter with  $\gamma = 2/3$  (plot d) has the flattest error around the origin. `findif-laplace` [CR]

where  $N_x$  is the helix period (the number of grid points in the  $x$  dimension). To find the inverse of a convolution with filter (B-9), we factorize the filter into the causal minimum-phase component and its adjoint:

$$F_9(Z) = P(Z)P(1/Z). \quad (\text{B-10})$$

To find the coefficients of the filter  $P$ , any one-dimensional spectral factorization method can be applied. It is important to point out that the result of factorization (neglecting the numerical errors) does not depend on  $N_x$ . Another approach is to define a residual error vector for the coefficients of  $Z$  in equation (B-10) and minimize it for some particular norm. For example, minimizing the  $\mathcal{L}_1$  norm when  $F_9$  is the McClellan filter (B-7), we discover that the filter  $P$ , after transforming back to two dimensions, takes the form

				-1.6094	0.4293	0.05157	0.017406	(B-11)
0.01428	0.033513	0.0808	0.2543	0.3521	0.1553			

The results of applying a recursive deconvolution with filter (B-11) are shown in Figure B-2. An essentially similar procedure, only with a different set of filters, works for implicit wavefield extrapolation.



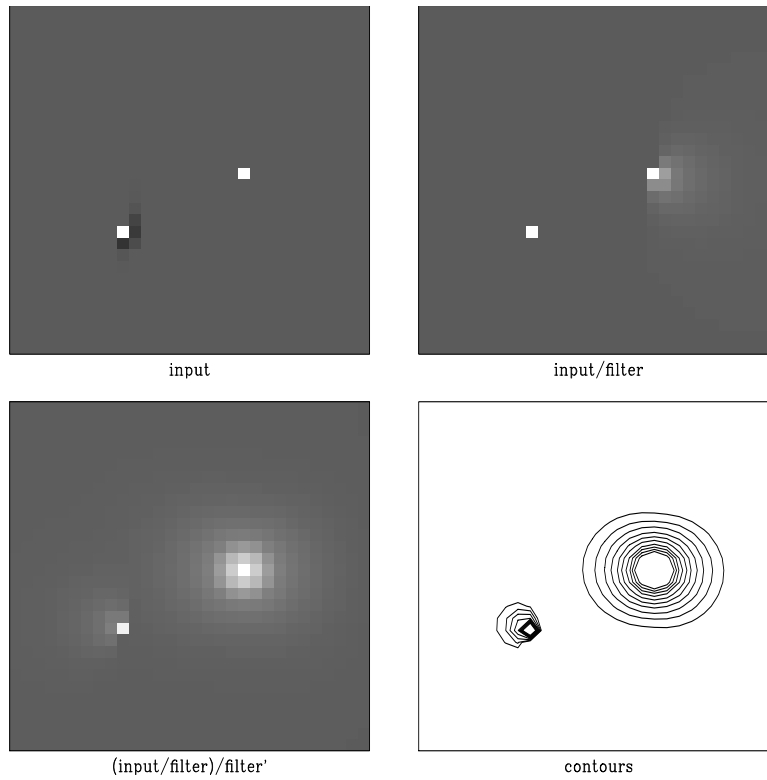


Figure B-2: Inverting the Laplacian operator by a helix deconvolution. The top left plot shows the input, which contains a single spike and the causal minimum-phase filter  $P$ . The top right plot is the result of inverse filtering. As expected, the filter is deconvolved into a spike, and the spike turns into a smooth one-sided impulse. After the second run, in the backward (adjoint) direction, we obtain a numerical solution of Laplace's equation! In the two bottom plots, the solution is shown with grayscale and contours. `findif-inv-laplace` [ER]

